HIGH FREQUENCY EFFECTS IN UNSTEADY ENTROPY MEASUREMENTS

Stephen J. Payne
Department of Engineering Science
University of Oxford
Oxford OX1 3PJ
sjp@robots.ox.ac.uk

ABSTRACT

Recent experimental measurements of unsteady entropy at exit from a high pressure turbine stage at engine-representative conditions have clearly shown that there are significant high frequency effects associated with the aspirating probe. This probe is the only current method of measuring entropy, which is vital in improving our understanding of unsteady flow fields, particularly the loss mechanisms. The two main high frequency effects, caused by the hot wires and the internal flow field, are examined here and their impact on the accuracy of unsteady entropy measurements presented. It is shown that the hot wire effects must be considered, but can be compensated for, whereas the internal flow field effects severely limit the performance of the aspirating probe.

INTRODUCTION

The flow fields inside turbomachines are still far from being understood thoroughly, due to the high degree of unsteadiness and effects of blade row interaction found therein. There is still much experimental work to be performed on understanding the formation of loss and on quantifying its effects on the stage efficiency at engine-representative conditions.

Since efficiency is usually defined as the ratio of the actual work output to the isentropic work output, only rises in entropy can reduce the efficiency. As entropy is only generated by heat transfer or flow irreversibility, "the only rational measure of loss in an adiabatic machine is entropy creation", **Denton, 1993**.

Entropy is independent of the frame of measurement and can be converted to efficiency if only one other property of state is known:

$$\eta = \frac{1-\left(\left(p_{o2}/p_{o1}\right)e^{(s_2-s_1)/R}\right)^{\frac{\gamma-1}{\gamma}}}{1-\left(p_{o2}/p_{o1}\right)^{\frac{\gamma-1}{\gamma}}}. \qquad \mathbf{1}$$

However, it cannot be measured directly and only changes in entropy have any meaning:

$$\frac{s_2-s_1}{R} = \left(\frac{\gamma}{\gamma-1}\right)\ln\left(\frac{T_{o2}}{T_{o1}}\right) - \ln\left(\frac{p_{o2}}{p_{o1}}\right). \qquad \mathbf{2}$$

Thus to make accurate measurements of entropy, two properties of state must be measured simultaneously, both spatially and temporally, relative to a reference condition. Since the aspirating probe is currently the only means of simultaneously measuring total pressure and total temperature both spatially and temporally, it is the sole option for unsteady entropy measurements.

Experimental measurements of unsteady entropy have recently been made at exit from a high pressure turbine stage, **Payne, 2001**, and **Payne et al., 2002**. These clearly showed the loss structure and allowed the effects of different loss mechanisms on the stage efficiency to be quantified. However, these measurements also showed that there are significant high frequency effects associated with the aspirating probe. These are now presented in detail, following an outline of the working of the aspirating probe.

NOMENCLATURE

a	Overheat ratio
c	Specific heat capacity; Speed of sound
d	Diameter
h	Heat transfer coefficient
k	Thermal conductivity
l	Length
n	Constant
p	Pressure
s	Specific entropy
t	Time
u	Velocity
x	Length
A	Area
C	Constant
D	Constant
E	Voltage
F	Function
G	Sensitivity coefficient
I	Current
K	Constant

M	Mach number
Nu	Nusselt number
R	Gas constant
T	Temperature; Time constant
Z	Fluctuating component
α	Temperature coefficient of resistance
β	Constant
γ	Ratio of specific heats
η	Efficiency; Recovery factor
ρ	Density; Resistivity
τ	Overheat ratio
χ	Ratio of heat transfer terms
ω	Frequency

Subscripts:

a	Ambient
m	Mean
mf	Medium frequency
o	Total conditions
ref	Reference conditions
s	Supports
ss	Steady state
w	Wire
1	HP vane inlet conditions
2	HP rotor exit conditions

Superscripts:

–	Time mean
*	Choked
′	Fluctuating component

THE ASPIRATING PROBE

The aspirating probe, **Ng and Epstein, 1983**, essentially consists of two hot wires placed upstream of a choked orifice, Figure 1. By calculating the mass flow for a given total pressure, total temperature and Mach number, the mass flow at the choked orifice and the hot wire plane can be equated to give:

$$(\rho u)_w = \sqrt{\frac{\gamma}{R}} \frac{p_o}{\sqrt{T_o}} \frac{A^*}{A_w} \left(\frac{2}{\gamma+1} \right)^{\frac{(\gamma+1)}{2(\gamma-1)}}. \qquad \mathbf{3}$$

Since the Mach number at the hot wire plane is fixed by the area ratio:

$$M_w \left(1 + \frac{\gamma-1}{2} M_w^2 \right)^{-\frac{(\gamma+1)}{2(\gamma-1)}} = \frac{A^*}{A_w} \left(\frac{\gamma+1}{2} \right)^{-\frac{(\gamma+1)}{2(\gamma-1)}}, \quad \mathbf{4}$$

the heat transfer coefficient is only dependent upon the Reynolds number, which in turn is only dependent upon the total pressure and total temperature. This gives the standard calibration equation for hot wire *i*:

$$E_i^2 = C_i \left(\frac{p_o}{\sqrt{T_o}} \right)^{n_i} \left(T_{wi} - \eta_i T_o \right). \qquad \mathbf{5}$$

The recovery factor, η, is the ratio of recovery temperature to total temperature and *C*, *D* and *n* are constants. These constants are all found by calibration, despite η being a known function of Mach number, to give the greatest accuracy. Two hot wires inside the aspirating probe thus yield two simultaneous equations in total pressure and total temperature, which can easily be solved to give total pressure and total temperature and hence entropy.

HOT WIRE FREQUENCY RESPONSE

The frequency response of a hot wire is found by analysing the general hot wire equation, for example **Højstrup et al., 1976**:

$$K_1 \frac{\partial T_w}{\partial t} = \frac{\partial^2 T_w}{\partial x^2} - \beta_1 T_w + K_2 T_a - K_3, \qquad \mathbf{6}$$

where the constants are given by:

$$K_1 = \frac{\rho_w c_w}{k_w}, \qquad \mathbf{7}$$

$$\beta_1 = \frac{h \pi d}{k_w A} - \frac{\alpha I^2 \rho_{ref}}{k_w A^2}, \qquad \mathbf{8}$$

$$K_2 = \frac{h \pi d}{k_w A}, \qquad \mathbf{9}$$

$$K_3 = \frac{I^2 \rho_{ref}}{k_w A^2} \left(\alpha T_{ref} - 1 \right). \qquad \mathbf{10}$$

The two main assumptions made are that the radial variations in wire temperature and the radiation heat transfer have negligible effect on the accuracy of the solution, **Payne, 2001**.

The complete solution to equation 6 requires the variation of all the parameters that depend upon the flow field: the current, heat transfer coefficient, flow temperature and wire temperature distribution. It is thus linearised about the steady state value by assuming small fluctuations to give:

$$\begin{aligned} \overline{K}_1 \frac{\partial T_w'}{\partial t} = \frac{\partial T_w'}{\partial x^2} - \overline{\beta}_1 T_w' - \beta_1' \overline{T}_w \\ + \overline{K}_2 T_a' + K_2' \overline{T}_a - K_3' \end{aligned} \qquad \mathbf{11}$$

Each component is assumed to vary sinusoidally:

$$\frac{T_w'}{\overline{T}_w} = Z_w e^{jwt}, \qquad \mathbf{12}$$

$$\frac{T_a'}{\overline{T}_a} = Z_a e^{jwt}, \qquad \mathbf{13}$$

$$\frac{h'}{\overline{h}} = Z_h e^{jwt}, \qquad \mathbf{14}$$

$$\frac{I'}{\overline{I}} = Z_I e^{jwt}, \qquad \mathbf{15}$$

giving an equation of the form:

$$Z_I = G_a(j\omega) Z_a + G_h(j\omega) Z_h, \qquad \mathbf{16}$$

where $G_a(j\omega)$ and $G_h(j\omega)$ are given at the end as equations 17 and 18. The following definitions are used:

$$\bar{\beta}_{11} = \bar{\beta}_1 + j\omega\bar{K}_1, \quad \textbf{19}$$

$$F(j\omega) = \frac{Z_w(x=\pm l)}{Z_a}, \quad \textbf{20}$$

$$\omega' = \omega\frac{\bar{K}_1}{\bar{\beta}_1}, \quad \textbf{21}$$

$$\xi_1 = \sqrt{\bar{\beta}_1}l\coth\left(\sqrt{\bar{\beta}_1}l\right), \quad \textbf{22}$$

$$\xi_{11} = \sqrt{\bar{\beta}_{11}}l\coth\left(\sqrt{\bar{\beta}_{11}}l\right), \quad \textbf{23}$$

$$a_{ref} = \alpha(T_m - T_{ref}), \quad \textbf{24}$$

$$a_a = \alpha(T_m - \bar{T}_a), \quad \textbf{25}$$

$$\tau = \frac{(T_m - \bar{T}_a)}{\bar{T}_a}. \quad \textbf{26}$$

Some simplifications can be made if it is assumed that $\sqrt{\beta_1}l$ is larger than approximately 3, i.e. that there is a reasonable amount of heat transfer. ξ_1 can be found from the overheat ratio if the ratio of heat transfer by conduction to heat transfer by convection:

$$\chi = \frac{d}{2l}\sqrt{\frac{k_w}{kNu}}, \quad \textbf{27}$$

is known. This gives:

$$\xi_1 = \frac{1}{\chi}\sqrt{\frac{(\xi_1 - 1)(1 + a_{ref} - a_a)}{(\xi_1 - 1)(1 + a_{ref} - a_a) + \xi_1 a_a}}, \quad \textbf{28}$$

which allows ξ_1 to be found iteratively once the overheat and heat transfer ratios are known. Equation 23 can also be simplified to give:

$$\xi_{11} = \xi_1\sqrt{1 + \omega'}. \quad \textbf{29}$$

However, since the hot wire is calibrated at zero frequency, the predicted steady state behaviour must be examined, since this determines the reference behaviour with which the general frequency response must be compared. We define the reference temperature to be equal to the ambient temperature to simplify the analysis. By letting the frequency tend to zero in equations 17 and 18:

$$(G_a)_{ss} = -\frac{(\xi_1 - 1)^2}{\tau}\frac{(1+a)}{\left[2(\xi_1 - 1)^2 + \xi_1 a(2\xi_1 - 3)\right]}, \quad \textbf{30}$$

$$(G_h)_{ss} = \frac{((\xi_1 - 1) + \xi_1 a)(2\xi_1 - 3)}{2\left[2(\xi_1 - 1)^2 + \xi_1 a(2\xi_1 - 3)\right]}. \quad \textbf{31}$$

The changes in sensitivity coefficients relative to the steady state are given at the end as equations 32 and 33.

There are thus only four dependent parameters: the overheat ratio (a), the frequency response of the supports ($F(j\omega)$), the ratio of heat transfer terms (χ) and the non-dimensional frequency (ω'). The parameter used to non-dimensionalise the frequency, equation 21, represents the attenuation frequency of the heat waves along the wire, and can be thought of as the time constant of the wire, T_w, reduced by the factor ξ_1^2 due to the feedback loop:

$$\frac{\bar{K}_1}{\bar{\beta}_1} = \frac{\rho_w c_w l^2}{k_w \xi_1^2} = \frac{T_w}{\xi_1^2}. \quad \textbf{34}$$

The frequency response of the hot wire supports is assumed to be a simple low-pass filter, as in **Højstrup et al., 1976**, **Freymuth, 1979**, and **Parantheon et al., 1983**:

$$F(j\omega) = \frac{1}{1 + j\omega T_s}. \quad \textbf{35}$$

The time constant is typically taken to be 1 second and this value has also been adopted here: its precise value is relatively unimportant, since the corresponding break frequency is much lower than most experimental measurements of interest.

Equations 32 and 33 are shown in Figure 2 for typical flow conditions and varying overheat ratio. The flow field is that in which the experimental measurements in **Payne et al., 2002**, were made: total pressure of 3.25 bar, total temperature of 297 K, Mach number of 0.45 with wire diameter and length of 5 μm and 1.2 mm. This gives a heat transfer ratio of 0.1390 and we set the time constants to be 0.001288 s and 1 s for the wire and the supports respectively.

There are two break frequencies, one due to the attenuation of heat transfer to the supports, and the other due to the attenuation of heat waves along the wire. The first only affects the sensitivity to temperature fluctuations and occurs at approximately 1 Hz, but the second affects both sensitivities. Although it starts to occur at approximately 10 kHz, its effects last until approximately 1MHz. The phase errors are negligible.

Since most experimental frequencies lie between the two break frequencies, the plateau level in this region is of greatest interest. Although the heat transfer sensitivity coefficient remains unchanged, the temperature sensitivity coefficient is:

$$\frac{(G_a)_{mf}}{(G_a)_{ss}} = \frac{((\xi_1 - 1) + \xi_1 a)}{\xi_1(1 + a)}. \quad \textbf{36}$$

This is almost independent of the overheat ratio and the difference between this value and the ideal value is approximately equal to the heat transfer ratio, χ. For given flow conditions this difference can only be reduced by an increase in the length/diameter ratio. Since this reduces the spatial resolution, some compromise is inevitable.

We now apply the general hot wire results to the aspirating probe, using equation 5. The sensitivity of hot wire voltage to changes in total pressure and total temperature is:

$$Z_{Ei} = \frac{n_i}{2} Z_{p_o} + \left(-\frac{n_i}{4} - \frac{1}{2\tau_i} \right) Z_{T_o}, \qquad \textbf{37}$$

where:

$$\tau_i = \frac{\dfrac{T_{wi}}{\overline{T_o}} - \overline{\eta_i}}{\overline{\eta_i}}, \qquad \textbf{38}$$

similar to equation 26. Since the values of n_i and τ_i are found by calibration at zero frequency, the changes with frequency result in:

$$Z_{Ei} = \left[\frac{n_i}{2} \frac{G_{hi}(j\omega)}{(G_{hi})_{ss}} \right] Z_{p_o} + \left[-\frac{n_i}{4} \frac{G_{hi}(j\omega)}{(G_{hi})_{ss}} - \frac{1}{2\tau_i} \frac{G_{ai}(j\omega)}{(G_{ai})_{ss}} \right] Z_{T_o}, \qquad \textbf{39}$$

where the transfer functions are given in equations 32 and 33 at the end.

By solving the equations for the two hot wire voltages simultaneously, the fluctuations in total pressure and total temperature can be found as functions of the voltage fluctuations:

$$Z_{p_o} = \frac{\tau_1(2 + n_2\tau_2)}{(n_1\tau_1 - n_2\tau_2)} Z_{E1} + \frac{\tau_2(2 + n_1\tau_1)}{(n_2\tau_2 - n_1\tau_1)} Z_{E2}, \qquad \textbf{40}$$

$$Z_{T_o} = \frac{2n_2\tau_1\tau_2}{(n_1\tau_1 - n_2\tau_2)} Z_{E1} + \frac{2n_1\tau_1\tau_2}{(n_2\tau_2 - n_1\tau_1)} Z_{E2}. \qquad \textbf{41}$$

These then give a sensitivity of entropy to changes in wire voltages:

$$\frac{s'}{R} = G_{s1} \frac{E_1'}{\overline{E_1}} + G_{s2} \frac{E_2'}{\overline{E_2}}, \qquad \textbf{42}$$

where:

$$G_{s1} = \frac{\tau_1(n_2\tau_2(\gamma+1) - 2(\gamma-1))}{(\gamma-1)(n_1\tau_1 - n_2\tau_2)} \qquad \textbf{43}$$

$$G_{s2} = \frac{\tau_2(n_1\tau_1(\gamma+1) - 2(\gamma-1))}{(\gamma-1)(n_2\tau_2 - n_1\tau_1)}. \qquad \textbf{44}$$

An absolute error must be given, since entropy has no absolute reference level.

Since the sensitivity to flow fluctuations varies with frequency, using a steady state calibration will inevitably incur errors when measuring the flow parameters at any significant frequency. Since this is somewhat intractable analytically, it will now be examined numerically.

We generate a flow field similar to that found at exit from a high pressure turbine stage by **Payne et al., 2002**. The fundamental rotor passing frequency is 8.91 kHz and the fluctuations in total pressure and total temperature are largely isentropic with a wake at approximately 60 % rotor passing generating most entropy. We assume that the flow field is measured with an aspirating probe of the dimensions given above, operating at overheat ratios of 0.2 and 1.0, the minimum and maximum allowable in practice. Hot wire voltages are generated using the high frequency analysis given above and then converted back to total pressure and total temperature using the uncorrected calibration.

The resulting entropy is shown in Figure 3 in comparison with the original plot. There is a noticeable difference between the two, showing that there is a significant high frequency effect, although it is reassuring that the difference is not such as to swamp the fluctuations in the signal. This effect must be compensated for using the theory above, but it does not cause a catastrophic effect in measuring unsteady entropy.

FLOW FIELD EFFECTS

Having examined the high frequency effects of the hot wires inside the aspirating probe, the high frequency effects due to the flow field inside the aspirating probe will now be presented. These effects are due to the fact that the nozzle remains choked at all times, affecting the behaviour of the upstream flow field.

By considering conservation of mass, momentum and energy in an unsteady flow field, three general equations can be developed for one-dimensional unsteady flow in a duct of changing cross-sectional area, **Shapiro, 1957**:

$$\frac{\partial \rho}{\partial t} + \rho \frac{\partial u}{\partial x} + u \frac{\partial \rho}{\partial x} + \frac{\rho u}{A} \frac{\partial A}{\partial x} = 0, \qquad \textbf{45}$$

$$\frac{\partial u}{\partial t} + u \frac{\partial u}{\partial x} + \frac{1}{\rho} \frac{\partial p}{\partial x} = 0, \qquad \textbf{46}$$

$$\frac{\partial p}{\partial t} + u \frac{\partial p}{\partial x} - c^2 \left(\frac{\partial \rho}{\partial t} + u \frac{\partial \rho}{\partial x} \right) = 0. \qquad \textbf{47}$$

Each flow property is split into its time-mean and time-varying components, assuming that the time-varying component is much smaller than the time-mean component. The time-mean equations reduce to:

$$\overline{\rho} \frac{\partial \overline{u}}{\partial x} + \overline{u} \frac{\partial \overline{\rho}}{\partial x} + \frac{\overline{\rho u}}{A} \frac{\partial A}{\partial x} = 0, \qquad \textbf{48}$$

$$\overline{u} \frac{\partial \overline{u}}{\partial x} + \frac{1}{\overline{\rho}} \frac{\partial \overline{p}}{\partial x} = 0, \qquad \textbf{49}$$

$$\frac{\partial \overline{p}}{\partial x} - c^2 \frac{\partial \overline{\rho}}{\partial x} = 0. \qquad \textbf{50}$$

These can be integrated to give the standard equations for conservation of mass, total temperature and entropy with distance, or re-arranged into the form:

$$\frac{1}{\overline{u}} \frac{\partial \overline{u}}{\partial x} = \frac{1}{\overline{M}^2 - 1} \frac{1}{A} \frac{\partial A}{\partial x}, \qquad \textbf{51}$$

$$\frac{1}{\overline{\rho}} \frac{\partial \overline{\rho}}{\partial x} = \frac{-\overline{M}^2}{\overline{M}^2 - 1} \frac{1}{A} \frac{\partial A}{\partial x}, \qquad \textbf{52}$$

$$\frac{1}{\overline{p}} \frac{\partial \overline{p}}{\partial x} = \frac{-\gamma \overline{M}^2}{\overline{M}^2 - 1} \frac{1}{A} \frac{\partial A}{\partial x}. \qquad \textbf{53}$$

The differential equations for the fluctuating components can then be found by assuming sinusoidal variations, giving:

$$\frac{j\omega}{\bar{u}} Z_\rho + \frac{\partial}{\partial x}\left(Z_u + Z_\rho\right) = 0, \qquad \textbf{54}$$

$$\frac{j\omega}{\bar{u}} Z_u + \frac{\partial Z_u}{\partial x} + \frac{1}{\gamma \bar{M}^2}\frac{\partial Z_p}{\partial x} + \frac{1}{\bar{M}^2 - 1}\frac{1}{A}\frac{\partial A}{\partial x}\left(2Z_u + Z_\rho - Z_p\right) = 0, \qquad \textbf{55}$$

$$\frac{j\omega}{\bar{u}}\left(Z_p - \gamma Z_\rho\right) + \frac{\partial}{\partial x}\left(Z_p - \gamma Z_\rho\right) = 0. \qquad \textbf{56}$$

In matrix form, these equations become:

$$\frac{\partial (Z)}{\partial x} + [T](Z) = 0, \qquad \textbf{57}$$

where:

$$(Z) = \begin{pmatrix} Z_u \\ Z_\rho \\ Z_p \end{pmatrix}, \qquad \textbf{58}$$

and the matrix T is given in equation 59 at the end.

Since the Mach number varies across the length of the tube, the solution is non-linear and must be solved numerically. However, at the throat, the Mach number tends to unity and thus the matrix T must be considered carefully. To prevent the matrix tending to infinity, the fluctuations must be in such a ratio that the matrix tends to zero instead. This can only be achieved when the fluctuations are in the ratios:

$$\left(Z^+\right) = \begin{pmatrix} Z_u^+ \\ Z_\rho^+ \\ Z_p^+ \end{pmatrix} = \begin{pmatrix} 1 \\ \gamma - 2 \\ \gamma \end{pmatrix} Z_u^+ . \qquad \textbf{60}$$

Since the aspirating probe is primarily used to measure entropy, via total pressure and total temperature, the relationship between the three properties of state used thus far and the Mach number, total pressure and total temperature is required:

$$\begin{pmatrix} Z_M \\ Z_{T_o} \\ Z_{p_o} \end{pmatrix} = [C] \begin{pmatrix} Z_u \\ Z_\rho \\ Z_p \end{pmatrix}, \qquad \textbf{61}$$

where:

$$[C] = \begin{pmatrix} 1 & \frac{1}{2} & -\frac{1}{2} \\ \frac{(\gamma-1)\bar{M}^2}{\phi} & \frac{-1}{\phi} & \frac{1}{\phi} \\ \frac{\gamma \bar{M}^2}{\phi} & \frac{\gamma \bar{M}^2}{2\phi} & \frac{1}{\phi}\left(1 - \frac{\bar{M}^2}{2}\right) \end{pmatrix}, \qquad \textbf{62}$$

$$\phi = 1 + \frac{(\gamma-1)\bar{M}^2}{2}. \qquad \textbf{63}$$

Hence, at the throat:

$$\begin{pmatrix} Z_M^+ \\ Z_{T_o}^+ \\ Z_{p_o}^+ \end{pmatrix} = \begin{pmatrix} 0 \\ 2 \\ \gamma \end{pmatrix} Z_u^+ . \qquad \textbf{64}$$

The ratio between total pressure and total temperature fluctuations at the throat is $\gamma/2$, in comparison to an isentropic ratio of $\gamma/(\gamma-1)$. This ratio is independent of the fluctuations at inlet to the probe and thus provides a severe restraint on the behaviour of the probe.

Although the hot wires are upstream of the throat, the flow field is set by the area variation and the frequency of oscillation. This can only be found numerically, but is simplified by the linearity of the model and the fixed relationships between the variables at the throat. For a fixed geometry and frequency, a small fluctuation in Z_u^+ is set up at the throat and the flow field solved backwards towards the entrance. The differential at the throat is:

$$\frac{\partial (Z)}{\partial x} = \frac{-j\omega}{\bar{u}} \begin{pmatrix} 1 \\ \gamma - 3 \\ 0 \end{pmatrix} Z_u^+ . \qquad \textbf{65}$$

Since the solution is linear, any differences in the magnitude and phase of Z_u^+ merely adjust the magnitude and phase of all the other parameters equally.

The quantity in which we are most interested is the ratio of total pressure fluctuations to total temperature fluctuations at the hot wire plane. For a probe with internal diameters 1 mm and 1.2 mm at the throat and hot wire planes respectively (corresponding to an inlet Mach number of 0.45), the magnitude and phase of this ratio are shown in Figure 4. A numerical solver was run in Matlab with 300 randomly generated frequencies in the range 1 kHz to 100 kHz. At low frequencies, the ratio is very close to $\gamma/2$, but it increases rapidly with frequency, as does the phase. Interestingly, there is a range of possible solutions over most frequencies. This is a characteristic of the non-linearity of the solution: although the equations were linearised in the fluctuating parameters, equation 57 is non-linear.

However, this range is small and the performance of the aspirating probe is severely limited by this restriction. In particular, it is not possible to measure over a wide range of total pressure and total temperature fluctuations, as the flow field inside the probe 'adjusts' the magnitude and phase of any fluctuations to the values shown in Figure 4. Some prior knowledge is thus required about the flow field to measure unsteady entropy accurately: this was possible in **Payne et al., 2002**, as previous experimental measurements of unsteady total pressure were available.

SUMMARY AND CONCLUSIONS

There are two high frequency effects involved in the aspirating probe: one due to the attenuation of heat transfer in the hot wires and supports and one due to the attenuation of flow field fluctuations inside the probe. The first effect has been analysed and a compensation factor derived, allowing measurements to be corrected: the effect is also relatively small, which prevents the errors from becoming significant. However, the second effect is much more significant, as the fluctuations in total pressure and total temperature are largely fixed by the geometry of the probe. This provides a severe restraint on the performance of the probe and prevents it from being used without some other knowledge of the flow field. The aspirating probe should thus be used with great care when making unsteady entropy measurements.

ACKNOWLEDGMENTS

The author wishes to thank Professor Roger Ainsworth and Dr. Robert Miller for many helpful discussions on this topic during his doctoral studies in Oxford.

REFERENCES

Denton, J.D. Loss mechanisms in turbomachines. *ASME Paper No. 93-GT-435*, 1993.

Freymuth, P. Engineering estimate of heat conduction loss in constant temperature thermal sensors. *TSI Quarterly*, 5: 3-9, 1979.

Højstrup, J., Rasmussen, K. and Larsen, S.E. Dynamic calibration of temperature wires in still air. *DISA Information*, 20: 22-30, 1976.

Ng, W.F. and Epstein, A.H. High-frequency temperature and pressure probe for unsteady compressible flows. *Review of Scientific Instruments*, 54: 1678-1683, 1983.

Parantheon, P., Lecordier, J.C. and Petit, C. Dynamic sensitivity of the constant-temperature hot-wire anemometer to temperature fluctuations. *TSI Quarterly*, 9: 3-8, 1983.

Payne, S.J. Unsteady loss in a high pressure turbine stage. D.Phil. Thesis, University of Oxford, 2001.

Payne, S.J., Ainsworth, R.W., Miller, R.J., Moss, R.W. and Harvey, N.W. Unsteady loss in a high pressure turbine stage. *To be submitted to International Journal of Heat and Fluid Flow*, 2002.

Shapiro, A.H. The dynamics and thermodynamics of compressible fluid flow: Volume 2. Wiley and Sons, 1957.

$$G_a(j\omega) = -\frac{1}{2\tau}\frac{(\xi_1-1)^2\, j\omega'\left[F(1+j\omega')(1+a_{ref}-a_a)+\left(\frac{\xi_{11}-1}{\xi_1-1}\right)\left((\xi_1-1)(1+a_{ref}-a_a)+\xi_1 a_a\right)\right]}{\xi_1\left[(1+j\omega')a_a(\xi_1-\xi_{11})+j\omega'(\xi_{11}-1)\left[(\xi_1-1)(1+a_{ref}-a_a)+\xi_1 a_a\right]\right]} \quad \textbf{17}$$

$$G_h(j\omega) = \frac{1}{2}\frac{\left[(\xi_1-1)(1+a_{ref}-a_a)+\xi_1 a_a\right]\left[(\xi_1-\xi_{11})+j\omega'\xi_{11}(\xi-1)\right]}{\xi_1\left[(1+j\omega')a_a(\xi_1-\xi_{11})+j\omega'(\xi_{11}-1)\left[(\xi_1-1)(1+a_{ref}-a_a)+\xi_1 a_a\right]\right]} \quad \textbf{18}$$

$$\frac{G_a(j\omega)}{G_{a,ss}} = \frac{1}{2}\frac{\left[2(\xi_1-1)^2+\xi_1 a(2\xi_1-3)\right]j\omega'\left[F(1+j\omega')+\left(\frac{\xi_{11}-1}{\xi_1-1}\right)\left((\xi_1-1)+\xi_1 a\right)\right]}{\xi_1(1+a)\left[(1+j\omega')a(\xi_1-\xi_{11})+j\omega'(\xi_{11}-1)\left[(\xi_1-1)+\xi_1 a\right]\right]} \quad \textbf{32}$$

$$\frac{G_h(j\omega)}{G_{h,ss}} = \frac{\left[2(\xi_1-1)^2+\xi_1 a(2\xi_1-3)\right]\left[(\xi_1-\xi_{11})+j\omega'\xi_{11}(\xi-1)\right]}{\xi_1(2\xi_1-3)\left[(1+j\omega')a(\xi_1-\xi_{11})+j\omega'(\xi_{11}-1)\left[(\xi_1-1)+\xi_1 a_a\right]\right]} \quad \textbf{33}$$

$$[T] = \left(\frac{\overline{M}^2}{\overline{M}^2-1}\right)\left[-\frac{j\omega}{\overline{u}}\begin{pmatrix} 1 & 0 & -\frac{1}{\gamma\overline{M}^2} \\ -1 & 1-\frac{1}{\overline{M}^2} & \frac{1}{\gamma\overline{M}^2} \\ -\gamma & 0 & 1 \end{pmatrix} + \frac{1}{\overline{M}^2-1}\frac{1}{A}\frac{\partial A}{\partial x}\begin{pmatrix} 2 & 1 & -1 \\ -2 & -1 & 1 \\ -2\gamma & -\gamma & \gamma \end{pmatrix}\right] \quad \textbf{59}$$

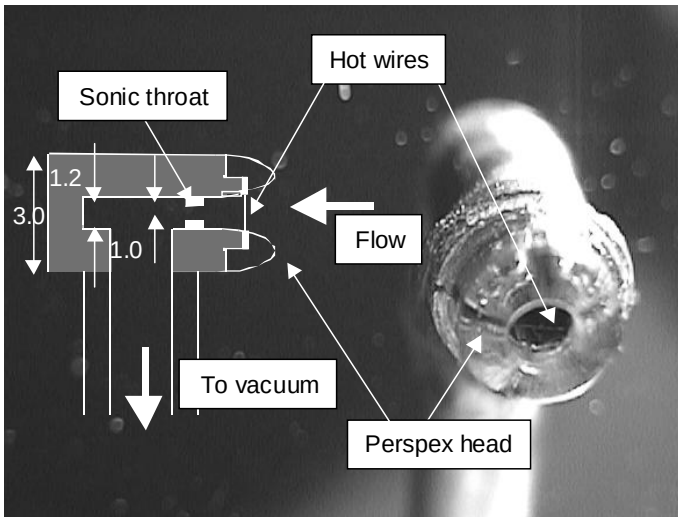

Figure 1 Oxford aspirating probe design, dimensions in mm

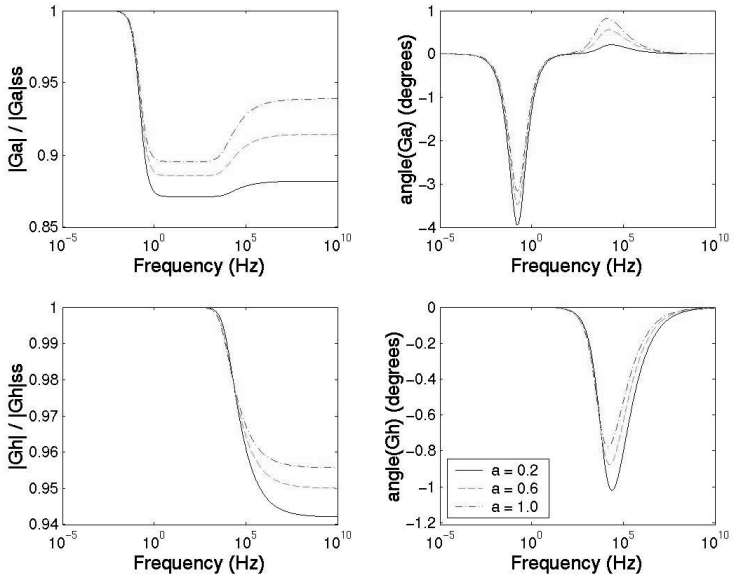

Figure 2 Variation of sensitivity coefficients with frequency (*f*) and overheat ratio (*a*)

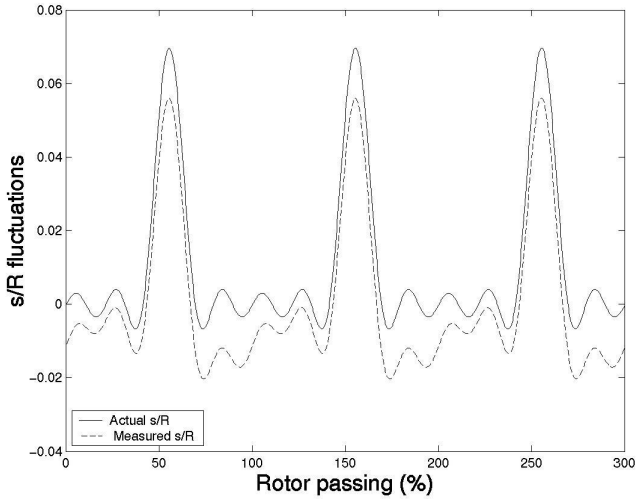

Figure 3 Unsteady entropy: comparison of measured fluctuations with actual fluctuations

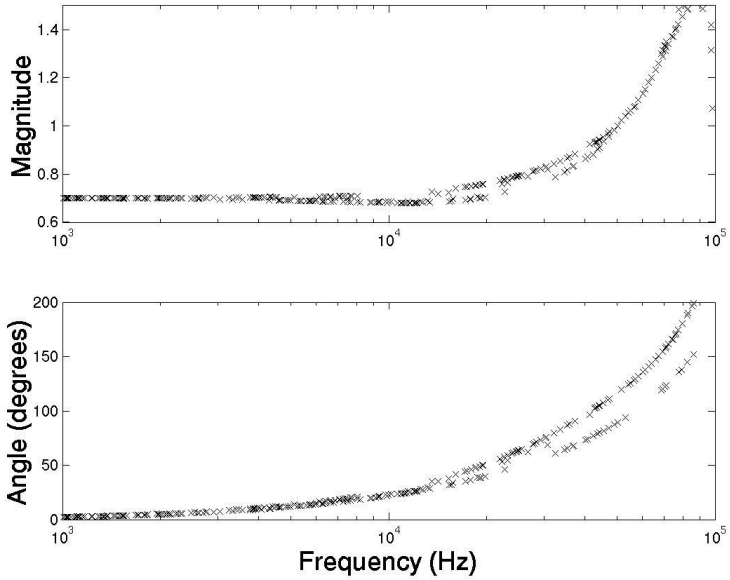

Figure 4 Magnitude and phase of ratio of total pressure/total temperature fluctuations